

https://doi.org/10.1070/QEL16659

Determination of characteristics of a magneto-optical trap by the spectral width of coherent two-photon resonance

A.A. Bobrov, S.A. Saakyan, V.A. Sautenkov, E.V. Vilshanskaya,
B.V. Zelener, B.B. Zelener

Abstract. **A technique is proposed for studying the thermal motion of ^{7}Li atoms in a magneto-optical trap (MOT), based on a comparative analysis of coherent two-photon resonances at the 2S–2P–*n*S (*n* = 38–120) transition using counter- and co-propagating laser beams with wavelengths of 671 and 350 nm (differential two-photon spectroscopy). A self-consistent theoretical model is constructed. The dependences of the broadening of two-photon resonance on the frequency detuning of cooling optical beams in the MOT are presented. A good agreement of theory with experimental results is obtained. The developed technique is nondestructive and can be used to determine the parameters of cold atoms in various traps, including the parameters of hydrogen and antihydrogen atoms in magnetic traps.**

Keywords: *laser cooling, Rydberg atoms, two-photon absorption, spectral line widths.*

1. Introduction

Methods of laser cooling and trapping of atoms in magneto-optical traps (MOTs) are widely used in modern technologies and basic research. Such traps are used as a source of cold atoms [1] in solving many problems from quantum computer science [2] to metrology [3,4]. Many experiments require an initially high phase density of atoms in the MOT for the subsequent production of the Bose–Einstein condensate [5,6] and the preparation of dense strongly interacting ensembles of Rydberg atoms [7]. To optimise MOT parameters, it is important to be able to perform a convenient optical diagnostics of such characteristics as the temperature of atoms and field broadening of atomic transitions caused by the action of optical cooling beams.

We have developed a simple nondestructive technique based on the analysis of two-photon excitation spectrum of ^{7}Li Rydberg atoms. The spectral lines were obtained by recording the variation of the fluorescence signal of cold atoms in the MOT. In work [8], a two-step (incoherent) excitation spectrum of ^{7}Li atoms in the MOT was investigated. As the first stage, laser beams from the MOT were used, and at the second stage use was made of UV radiation from a laser system (radiation from a tunable frequency-doubled Ti:sapphire laser). When the frequency of UV laser radiation coincided with the frequency of the Rydberg transition, narrow dips in fluorescence of the cloud of cold atoms were observed. High contrast of the thus obtained resonances was determined, on the one hand, by a low pump rate of the atoms in the MOT, and on the other hand, by a relatively high escape rate of the Rydberg atoms from the cloud. In work [9], a higher spectral resolution of the two-photon resonance line was obtained by reducing the scanning rate of the UV radiation frequency. Using the technique proposed, it was possible to investigate both dipole-resolved and forbidden atomic transitions [10–14]. Using two-photon spectroscopy, the ^{7}Li ionisation threshold was measured [11,12], and also quantum defects for the Rydberg states *n*S [11], *n*P [12], *n*D [10] and *n*F [13] were determined.

In our paper [15], we investigated coherent two-photon resonances in ^{7}Li. For coherent excitation, radiation of a red laser was used as the first stage, the frequency of which was detuned from the $2S(F = 2)–2P_{3/2}(F = 3)$ resonance by –0.59 GHz. The UV laser frequency detuning from the $2P_{3/2}$ (F = 3)–*n*l transition was scanned in the vicinity of +0.59 GHz. When the coherent two-photon transition condition was satisfied, we were able to record very narrow resonances; the smallest recorded width constituted 4.4 MHz, which is much less than the width of incoherent resonances (~100 MHz) we had previously obtained. The small spectral width of resonances is explained by the exclusion of the 2P level width for a completely coherent process. Coherent spectroscopy allows nondestructive determination of various MOT characteristics, including the field broadening, the temperature of atoms, and the effect of electric and magnetic fields.

In the present work, a technique is developed for determining the temperature of ^{7}Li atoms in the MOT and the effect of MOT beams on the widths of transitions. This technique is based on a comparative analysis of spectral lines of coherent two-photon resonances for the cases of co- or counterpropagating beams of red and UV lasers. Section 2 describes the experimental setup, the level diagram, and a method for UV laser stabilisation which makes it possible to achieve an effective line width of 0.2 MHz. In Section 3, in order to explain the experimental data obtained, a theoretical model is proposed that simultaneously takes into account both the Doppler and field contributions to the coherent resonance line broadening. Section 4 discusses the results of experiments and compares them with the results of calculations.

2. Experimental setup

A detailed description of the experimental setup for laser cooling and trapping of ^{7}Li atoms in the MOT can be found in [16, 17]. The vacuum system consists of a source of atomic

A.A. Bobrov, S.A. Saakyan, V.A. Sautenkov, E.V. Vilshanskaya, B.V. Zelener, B.B. Zelener Joint Institute for High Temperatures, Russian Academy of Sciences, ul. Izhorskaya 13, stroenie 2, 125412 Moscow, Russia, e-mail: abobrov@inbox.ru

Received 21 February 2018
Kvantovaya Elektronika **48** (5) 438–442 (2018)
Translated by M.A. Monastyrskiy

beam, a Zeeman slower, and a basic vacuum chamber. For laser cooling and trapping in the MOT, two semiconductor lasers with a wavelength of about 671 nm are used. Both lasers are stabilised by the resonances of saturated absorption in cells with ^{7}Li vapours. The hyperfine splitting of the ground state of the ^{7}Li atoms constitutes ~0.8 GHz, which necessitates the use of two laser sources.

The cooling laser is stabilised at the $2S_{1/2}$ (F = 2)–$2P_{3/2}$ (F = 3) transition frequency with the possibility of continuous radiation frequency detuning in stabilisation regime by a double-pass acousto-optic modulator (AOM) [18]. The optical pump (OP) laser is stabilised at the $2S_{1/2}$ (F = 1)–$2P_{3/2}$ (F = 3) transition frequency without radiation frequency modulation. To obtain the error signal, the frequency of the double-pass AOM is modulated.

Both sources of laser radiation have virtually the same output powers equal to 0.5 and 0.3 W for a cooling laser and an optical pump laser, respectively. In all MOT beams, 30% of intensity is provided by the OP laser and 70% of intensity – by the cooling laser. Both lasers participate in the cooling process and represent cooling lasers, but for convenience, and also by analogy with other MOT types, we will further refer to them as the cooling laser and the OP laser.

Figure 1 shows the level diagram of the ^{7}Li atom used to excite the Rydberg states. To this end, two counter- or co-propagating collinear laser beams with the wavelengths λ_1 = 671 and λ_2 = 350 nm are used (in Fig. 1b they are denoted as k_1 and k_2, respectively). A small part of radiation from the cooling laser is detuned from the transition frequency $2S_{1/2}$–$2P_{3/2}$ by –0.59 GHz and forms a red beam k_1. Radiation with a wavelength of 350 nm is obtained by doubling the radiation frequency of a Ti:sapphire laser. The frequency of the latter is stabilised using the Pound–Drever–Hall (PDH) technique [19] by the resonances of a thermally stabilised Fabry–Perot interferometer (FPI), whose length, in turn, is stabilised by the radiation of a cooling laser. The description of this UV laser system and the method of frequency stability transmission by the FPI can be found in [20].

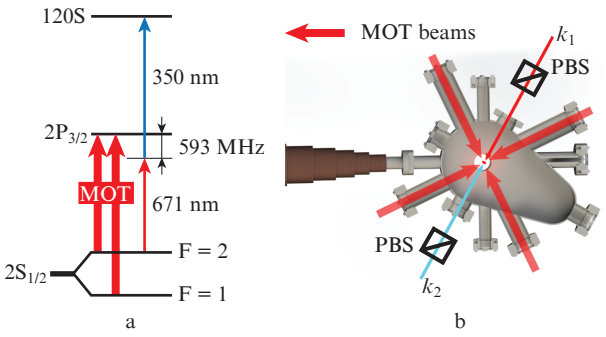

Figure 1. (a) Diagram of levels of the ^{7}Li atom used in the experiment and (b) schematic of the setup:
(PBS) polarisation beam splitter; (k_1) laser beam with λ_1 = 671 nm; (k_2) laser beam with λ_2 = 350 nm.

The energy spectrum of the Rydberg transitions was recorded by the method of a drop in resonance fluorescence of the atoms in the MOT. The UV laser radiation frequency was continuously tuned and measured using a calibrated Angstrom WS-U wavemeter. When the UV laser passed through the frequency of two-photon transition to the Rydberg states, a decrease in the fluorescence of the atoms in the MOT was observed. The cloud fluorescence intensity was recorded using a photodetector and a CCD camera. This method is described in detail in [8, 21].

Figure 2 shows the resonances at the $2S_{1/2}$–38S, $2S_{1/2}$–82S, and $2S_{1/2}$–120S transitions [15]. It is seen from the experiment that the width of coherent two-photon resonances in the nS state does not depend on the principal quantum number n. The natural width of the Rydberg levels is less than 3 kHz. In the case of two-photon coherent excitation, the natural width of the intermediate state $2P_{3/2}$ does not enter the width of the observed transition δ. Therefore, the width of the resonances is determined by the processes that take place in the trap, and in this paper we propose a technique that makes it possible to determine various characteristics of the MOT by analysing the spectral widths of the resonances.

Measurements of the spectral widths of laser radiation sources used to excite the Rydberg states of ^{7}Li atoms were carried out by means of a Sirah EagleEye commercial optical spectrum analyser [22], which includes a scanning interferometer and an electronic unit. A small part of radiation from a Ti:sapphire laser (700 nm wavelength before frequency doubling) was directed to the optical spectrum analyser. The line width analysis was carried out continuously in the course of all the experiments.

Figure 3a shows the time dependence of the emission spectrum width of a Ti:sapphire laser, measured with the EagleEye system. The average value of the instantaneous line width was ~0.1 MHz/100 ms. After frequency doubling, the

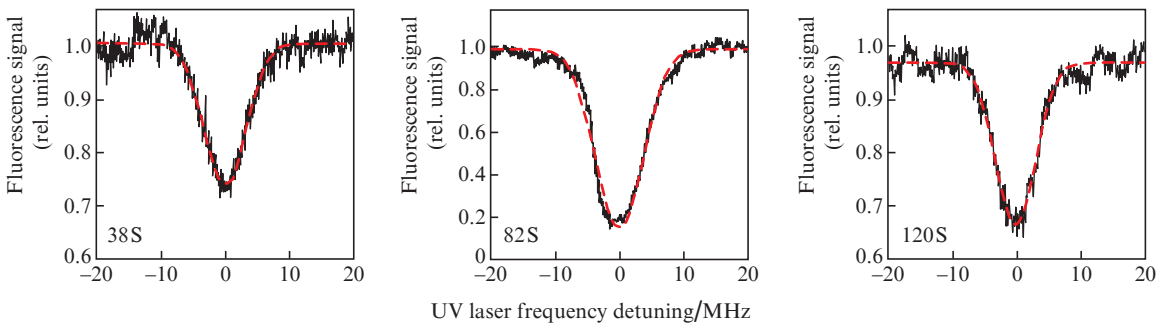

Figure 2. Different resonances at the transitions to nS states (dashed curve shows the fit by the Gauss function). Frequency detuning of the cooling laser is 13 MHz, the total intensity of the MOT beams is 50.4 mW cm^{-2}. State 38S: I_{350} = 196 mW cm^{-2}, I_{671} = 2.5 mW cm^{-2}, δ = 7.8 MHz; 82S: I_{350} = 147 mW cm^{-2}, I_{671} = 28 mW cm^{-2}, δ = 8.8 MHz; 120S: I_{350} = 176 mW cm^{-2}, I_{671} = 36 mW cm^{-2}, δ = 7.4 MHz.

spectrum width of the UV radiation exciting the Rydberg states was ~0.2 MHz.

The measured instantaneous emission line widths of the OP laser and the cooling laser were ~0.5 MHz/100 ms and ~0.22 MHz/100 ms, respectively.

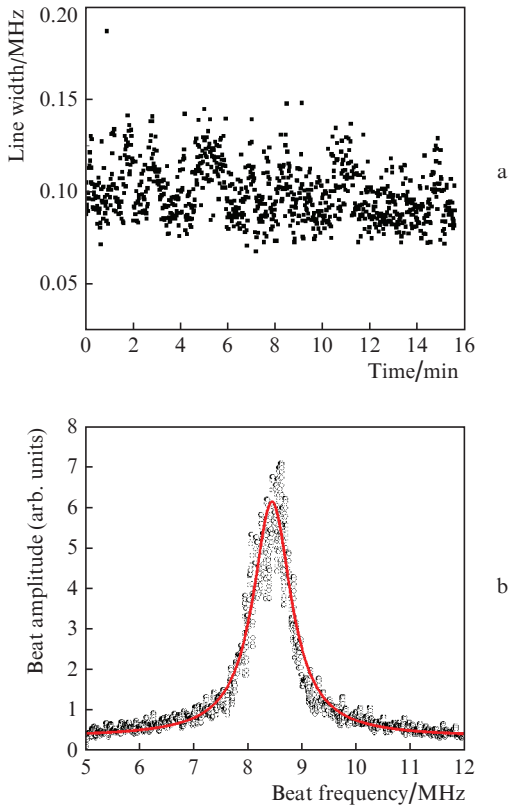

Figure 3. (a) Emission line width of a laser with a wavelength of 700 nm before frequency doubling that excites the Rydberg states of ^{7}Li atoms, and (b) beat signal of radiations from the pump laser and cooling laser (the dots are the experiment, the solid curve is the fit by the Lorentz function with a width of $\omega = 0.86$ MHz).

The independent measurements of the line widths of the pump laser and the cooling laser, carried out in accordance with their beats, made it possible to verify the correctness of the analyser readings and to estimate the total width of the emission lines of two lasers. The beat-frequency waveforms of the radiation from the OP and cooling lasers are shown in Fig. 3b. To observe the beats, both sources were stabilised at the $2S_{1/2}$ (F = 2)–$2P_{3/2}$ (F = 3) transition frequency in a cell with ^{7}Li vapours. Small discrepancies in the measurement results can be explained by the instability of the OP laser. Hence it can be concluded that the width of the observed resonances is due not only to the spectral width of the laser radiation, but also to other factors determined by the parameters of this trap, such as Doppler broadening, power and detuning of MOT beams, and magnetic field gradient.

3. Theoretical model

Let us consider a two-photon coherent 2S–2P –nl transition in a simple three-level approximation, in which the red laser field acts on the 2S–2P transition, and the UV laser field – on the 2P–nS (nD) transition. We neglect the hyperfine splitting of the ground state 2S and excited state 2P.

We use the density matrix formalism [23] for theoretical description of the experimental results. We denote the 2S level by 1, 2P by 2 and nS (nD) by 3. In our model, two plane waves propagate along the z axis (in parallel or opposite directions), and the atoms move with the velocities $\boldsymbol{u}$. The Doppler effect for the fields of red and UV lasers is introduced into the equations in the form of the frequency shifts $\delta_1 - k_{1z}u$ and $\delta_2 - k_{2z}u$, respectively, where $\delta_1 = -0.59$ GHz is the frequency detuning of the red laser from the transition 1–2; δ_2 is the frequency detuning of the UV laser from the transition 2–3; u is the projection of the velocity vector on the z axis (beam propagation axis); and k_{1z} and k_{2z} are the projections of the wave vectors on the z axis. The Rabi frequencies for these transitions are $\Omega_i = d_i E_i/\hbar$, where d_i are the matrix moments of dipole transitions and E_i are the amplitudes of the corresponding optical fields ($i = 1, 2$). Following [23], we can present the equations for the components of the density matrix $\{\rho_{ij}\}$ ($i,j = 1,2,3$) in the rotating wave approximation in the form

$$\dot\rho_{11} = 0.5\mathrm{i}\Omega_1(\rho_{21} - \rho_{12}) + 2\gamma_2\rho_{22} + \Gamma_{\mathrm{trap}}(1 - \rho_{11}),$$

$$\dot\rho_{22} = 0.5\mathrm{i}\Omega_1(\rho_{12} - \rho_{21}) - 2\gamma_2\rho_{22} + 0.5\mathrm{i}\Omega_2(\rho_{32} - \rho_{23}),$$

$$\dot\rho_{33} = 0.5\mathrm{i}\Omega_2(\rho_{23} - \rho_{32}) - 2\gamma_3\rho_{33} - \Gamma_{\mathrm{R}}\rho_{33},$$

$$\dot\rho_{12} = 0.5\mathrm{i}\Omega_1(\rho_{22} - \rho_{11}) - \rho_{12}[\gamma_2 + \mathrm{i}(\delta_1 - k_{1z}u)] - 0.5\mathrm{i}\Omega_2\rho_{13},$$

$$\dot\rho_{23} = 0.5\mathrm{i}\Omega_1(\rho_{33} - \rho_{22}) - \rho_{23}[\gamma_2 + \mathrm{i}(\delta_2 - k_{2z}u)] + 0.5\mathrm{i}\Omega_1\rho_{13},$$

$$\dot\rho_{13} = 0.5\mathrm{i}\Omega_1\rho_{23} - 0.5\mathrm{i}[\delta_1 + \delta_2 - (k_{1z} + k_{2z})u]\rho_{13} - 0.5\mathrm{i}\Omega_2\rho_{12} - \rho_{13}\gamma_{13},$$

$$\rho_{ij} = \rho^*_{ji}. \qquad (1)$$

Relaxation terms are added to the equations: Γ_{trap} is the rate of arrival/escape of atoms in the MOT; Γ_{R} is the rate of emission of Rydberg atoms from the trap; $2\gamma_2$ and $2\gamma_3$ are the rates of spontaneous decay of the 2P and nl states, respectively; and γ_{13} is the rate of coherence decay of the 2S–nl transition.

It should be noted that we consider an open system and the diagonal matrix elements have the meaning of the relative populations of levels; as a result, we have $\mathrm{Sp}\{\rho_{ij}\} \neq 1$.

Despite the fact that the radiation of MOT beams does not directly affect the population kinetics of the Rydberg state, the field of cooling lasers broadens the spectral width of the 2S state (field broadening γ_{f}), which, in turn, leads to the coherence destruction of the ground and Rydberg states. The rate of coherence destruction γ_{13} is represented as the half-sum of the field broadening γ_{f}, the rate of spontaneous decay of the Rydberg state $2\gamma_3$, the escape rates of atoms in the ground state Γ_{trap}, and the escape rates of the Rydberg atoms Γ_{R}:

$$\gamma_{13} = 0.5(\gamma_{\mathrm{f}} + 2\gamma_3 + \Gamma_{\mathrm{trap}} + \Gamma_{\mathrm{R}}). \qquad (2)$$

In the two-level approximation, the field broadening can be estimated as

$$\gamma_{\mathrm{f}} = 2\gamma_2\frac{\Omega_{\mathrm{f}}^2/4}{\Delta^2 + 4\gamma_2^2 + \Omega_{\mathrm{f}}^2/4}, \qquad (3)$$

where Δ is the frequency detuning of the cooling laser from the 2S–2P transition and Ω_f is the Rabi frequency corresponding to this transition. The rate of spontaneous decay of the Rydberg states $2\gamma_3$ for the levels in question is about several kHz [24]. The loss rate of atoms in the ground state is $\Gamma_{trap} \approx 0.1$ Hz proceeding from the fact that the MOT loading rate is ~ 10 s. Given that the rate of atoms is 1 m s^{-1} and the atomic cloud size in the MOT is of the order of 1 mm, the escape rate Γ_R of the Rydberg atoms from the MOT can be estimated as 1 kHz. At the same time, for the lowest intensity of the MOT beams, the field broadening γ_f is approximately several hundred kHz, and, consequently, the field action of the MOT beams on the 2S–2P transition provides the main contribution to the homogeneous line broadening.

The results of the solution $\rho_{ij}(\delta_2, u)$ of system (1) should be averaged over the velocity distribution of atoms:

$$\rho_{ij}(\delta_2) = \int_{-\infty}^{+\infty} \rho_{ij}(\delta_2, u) \frac{1}{\sqrt{\pi}} \frac{1}{u_{th}} \exp\left(-\frac{u^2}{u_{th}^2}\right) du. \quad (4)$$

The thermal velocity u_{th} is expressed in terms of the temperature of atoms as follows:

$$u_{th} = \sqrt{2k_B T/m}, \quad (5)$$

where k_B is the Boltzmann constant and m is the atomic mass of ^{7}Li.

The temperature of atoms in the MOT can be expressed in terms of the detuning and intensity of the MOT laser beams in accordance with the Doppler theory [25], using the relation

$$k_B T = \frac{\hbar\gamma_2}{2} \frac{1 + I_{tot}/I_s + (\Delta/\gamma_2)^2}{|\Delta|/\gamma_2}, \quad (6)$$

where I_{tot} is the total intensity of the cooling beams; and $I_s = 2.5$ mW cm^{-2} is the saturation intensity of the 2S–2P transition.

The speed of frequency scanning of the UV laser in our experiments is sufficiently small, which allows us to consider the system as being in a stationary state for any detuning value δ_2. Therefore, we may assume the derivatives in the left-hand side of system (1) equal to zero and solve the system as an algebraic one. In work [23], a stationary solution of equation (1) is given in the first order of perturbation theory (in terms of the UV laser radiation intensity) for the case of large absolute values of δ_1 and δ_2:

$$\rho_{33}(\delta_2, u) \sim \frac{\Omega_1^2 \Omega_2^2 \gamma_{13}}{\gamma_3 \delta_1 \delta_2 [\delta_1 + \delta_2 - (k_{1z} + k_{2z})u]^2 + \gamma_{13}^2}. \quad (7)$$

Solution (7) represents a Lorentz function; averaging of this solution over the thermal distribution yields a Voigt profile, the contribution to the characteristic width (FWHM) of which is simultaneously given by the field and Doppler broadening. As can be seen from (7), the widths of the spectral lines of two-photon absorption for counterpropagating and co-propagating beams of red and UV lasers will be different, since the projections of the wave vectors on the z axis have opposite signs in the case of counterpropagating beams and identical signs in the case of co-propagating beams. In this case, the width difference depends exclusively on the temperature T of atoms. Since the first order of perturbation theory gives incorrect results at high UV laser radiation intensities, in Section 4 we give the results of numerical solution of equations (1).

4. Results and discussion

Figure 4 shows the experimentally obtained spectral contours of two-photon resonances 2S–2P–58S for various propagation directions of the beams. Figure 5a shows the width (FWHM) dependences of two-photon resonance on the frequency detuning of the MOT beams, obtained in the experiment and also by solving the equations for the density matrix elements $\rho_{11}(\delta_2)$. Good agreement between the experimental and theoretical results allows us to conclude that our assumptions regarding the effect of cooling optical MOT beams on the width of two-photon resonances are correct.

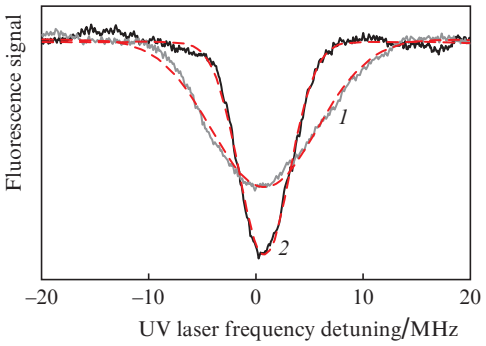

Figure 4. Two-photon resonances at the transitions to the 58S state in the case of (*1*) co-propagating and (*2*) counterpropagating exciting beams [solid curves is the experiments, dashed curves are the approximations by the Gauss function with the FWHM value equal to (*1*) 11.8 and (*2*) 5.7 MHz].

As was shown in Section 3, the difference in the resonance widths is only determined by the atomic cloud temperature. In some approximation, the temperature of the atoms can be estimated if we represent the resonance spectral width as a sum of the field broadening $\Delta\omega_f$ and the Doppler broadening. The field broadening does not depend on the propagation direction of the beams, while the Doppler broadening is determined by the difference in the wave numbers $2(\ln 2)\,(k_2 - k_1)u_{th}$ for counterpropagating beams and the sum of the wave numbers $2(\ln 2)\,(k_2 + k_1)u_{th}$ for co-propagating beams of the red and UV lasers. Let us determine the thermal broadening using the relation

$$\Delta\omega_{th} = 4\pi(\ln 2)(u_{th}/\lambda_1). \quad (8)$$

Using relations (5) and (8), we can determine the temperature and the field broadening $\Delta\omega_f$.

Figure 5b shows the experimental dependence of the field broadening $\Delta\omega_f$ on the frequency detuning of the cooling beams. The broadening $\Delta\omega_f$ is reduced to approximately 0.6 MHz with increasing detuning Δ to about 20 MHz, which agrees with formula (3). With a further increase in detuning, the broadening increases. The increase in broadening can be stipulated by an increase in the size of the atomic cloud (see Fig. 6a). This leads to the fact that atoms begin to experience the action of a strong magnetic field; given that the MOT field gradient is 21 G cm^{-1}, the broadening can amount to $\sim$1 MHz at the cloud size of 1 mm.

Figure 6b shows the results of measurements and calculations [using formula (6)] of the temperature of atoms on the basis of experimental data. Good agreement between theo-

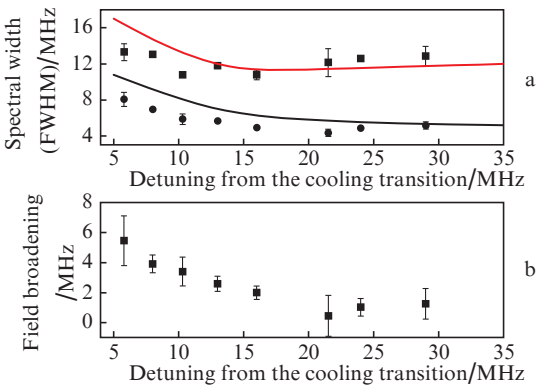

Figure 5. Dependences of (a) the spectral width of two-photon resonances at the transitions 58S and (b) field broadening $\Delta\omega_f$ on the frequency detuning of the MOT-forming beams from the $2S_{1/2}$ (F = 2)–$2P_{3/2}$ (F = 3) transition in the case of ($k_1 + k_2$) (■) co-propagating beams and (●) counterpropagating beams ($k_2 - k_1$); solid curves show the stationary solution of equations (1). The total intensity of the MOT beams is 42 mW cm^{-2}.

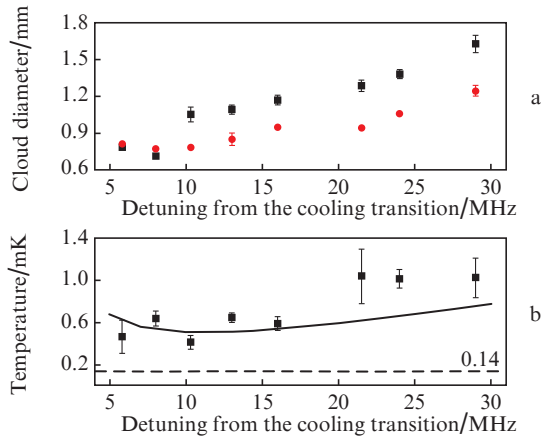

Figure 6. Dependences of (a) the cloud diameter along (■) the abscissa and (●) the ordinate axis and (b) the cloud temperature on the frequency detuning of the MOT-forming beams from the cooling transition $2S_{1/2}$ (F = 2)–$2P_{3/2}$ (F = 3) (points show the experiment, solid curve show the calculation). The dashed line shows the Doppler cooling limit for lithium atoms, equal to 0.14 mK.

retical and experimental dependences indicates the prospects of using differential two-photon spectroscopy proposed in this paper for measuring the temperature of atoms in the MOT.

We should note that in the experiment, we measured the width of an inhomogeneously broadened contour. Precise determination of the contributions of the field broadening and the broadening associated with the thermal motion of atoms assumes an analysis of the convolution of the Lorentz function (field broadening) and the Gauss function (Maxwellian distribution), and the solution of an inverse problem [26]. However, good agreement with theory makes it possible to use this approximate method for estimating the field broadening and temperature with sufficient degree of accuracy.

The temperature dependence of detuning is nonlinear and has an expressed minimum. Note that the temperature minimum is observed approximately with the same detuning value, at which we recorded the highest density of atoms in the trap [17].

5. Conclusions

Using the example of measuring the temperature of ^{7}Li atoms in an operating MOT, the application of difference two-photon spectroscopy for optical diagnostics of the parameters of trapped cold atoms is demonstrated. A self-consistent theoretical model describing the experimental results is proposed. The advantages of the method proposed in the work are the simplicity and nondestructive nature of the measurements. The technique can be used to optimise the MOT parameters; one of the interesting applications is determination of the parameters of a cloud of antihydrogen atoms in magnetic traps.

Acknowledgements. The authors thank L.G. Dyachkov for his help in calculating the matrix dipole transition moments for the ^{7}Li Rydberg states. The work was supported by the Russian Science Foundation (Grant No. 17-72-10285).

References

1. Dieckmann K. et al. *Phys. Rev. A*, **58**, 3891 (1998).
2. Beterov I.I., Saffman M., Yakshina E.A., et al. *Phys. Rev. A*, **88**, 010303 (2013).
3. Nicholson T.L., Campbell S.L., Hutson R.B., et al. *Nat. Commun.*, **6**, 6896 (2015).
4. Golovizin A.A. et al. *Quantum Electron.*, **45** (5), 482 (2015) [*Kvantovaya Elektron.*, **45** (5), 482 (2015)].
5. Chapovsky P.L. *Pis'ma Zh. Eksp. Teor. Fiz.*, **95** (3), 148 (2012).
6. Salomon G., Fouché L., Lepoutre S., et al. *Phys. Rev. A*, **90** (3), 033405 (2014).
7. McQuillen P., Zhang X., Strickler T., et al. *Phys. Rev. A*, **87** (1), 013407 (2013).
8. Zelener B.B., Saakyan S.A., Sautenkov V.A., et al. *Pis'ma Zh. Eksp. Teor. Fiz.*, **100** (6), 408 (2014).
9. Sautenkov V.A. et al. *J. Russ. Laser Res.*, **36** (2), 193 (2015).
10. Sautenkov V.A., Saakyan S.A., Vilshanskaya E.V., et al. *Laser Phys.*, **26**, 115701 (2016).
11. Zelener B.B., Saakyan S.A., Sautenkov V.A., et al. *Pis'ma Zh. Eksp. Teor. Fiz.*, **148**, 1086 (2015).
12. Zelener B.B., Saakyan S.A., Sautenkov V.A., et al. *Pis'ma Zh. Eksp. Teor. Fiz.*, **149**, 750 (2016).
13. Saakyan S.A., Sautenkov V.A., Zelener B.B. *J. Phys.: Conf. Ser.*, **774**, 012165 (2016).
14. Zelener B.B., Saakyan S.A., Sautenkov V.A., et al. *Dokl. Akad. Nauk*, **467**, 526 (2016).
15. Sautenkov V.A., Saakyan S.A., Vilshanskaya E.V., et al. *J. Russ. Laser Res.*, **38** (1), 91 (2017).
16. Zelener B.B., Saakyan S.A., Sautenkov V.A., et al. *Pis'ma Zh. Eksp. Teor. Fiz.*, **98**, 762 (2013).
17. Zelener B.B., Saakyan S.A., Sautenkov V.A., et al. *Zh. Eksp. Teor. Fiz.*, **146**, 909 (2014).
18. Donley E.A., Heavner T.P., Levi F., et al. *Rev. Sci. Instrum.*, **76** (6), 063112 (2005).
19. Drever R.W.P., Hall J.L., Kowalski F.V., et al. *Appl. Phys. B*, **31** (2), 97 (1983).
20. Saakyan S.A., Sautenkov V.A., Zelener B.B. *J. Phys.: Conf. Ser.*, **946**, 012128 (2018).
21. Saakyan S.A. et al. *Quantum Electron.*, **45** (9), 828 (2015) [*Kvantovaya Elektron.*, **45** (9), 828 (2015)].
22. Hädrich S., Jauernik P., McCrumb L., Feru P. *Proc. SPIE*, **6871**, 68711S-1 (2008).
23. Stenholm S. *Foundations of Laser Spectroscopy* (New York: John Wiley & Sons, Inc., 1984).
24. Theodosiou C.E. *Phys. Rev. A*, **30**, 2881 (1984).
25. Xu X., Loftus T.H., Smith M.J., et al. *Phys. Rev. A*, **66** (1), 011401 (2002).
26. Strickler T.S., Langin T.K., McQuillen P., et al. *Phys. Rev. X*, **6**, 021021 (2016).